Design of an all-normal dispersion photonic crystal fiber for stable and coherent supercontinuum generation

R. Morel[1], V. Thibaut[2], M. Marcadier[2,3], Y. Pertot[3], A. Jullien[2], N. Forget[2], A. Cassez[4], V. Andrieux[4], D. Labat[4], O. Vanvincq[4], A. Kudlinski[4], J. M. Dudley[1], and T. Sylvestre[1,*]

[1] Université Marie et Louis Pasteur, CNRS, FEMTO-ST, Besançon, France
[2] Université Côte d'Azur, CNRS, Institut de Physique de Nice (INPHYNI), Nice, France
[3] Fastlite by Amplitude Systems, Antibes, France
[4] Université de Lille, CNRS, PhLAM-Physique des Lasers Atomes et Molécules, Lille, France

ABSTRACT

We demonstrate a novel polarization-maintaining all-normal dispersion photonic crystal fiber (PM-ANDi PCF) engineered for femtosecond pumping at 1030 nm, enabling ultra-stable and highly coherent supercontinuum generation from 650 to 1300 nm. Polarization control is achieved through an innovative two-hole design that replaces traditional stress rods, offering simplicity and robustness. Numerical and experimental studies reveal excellent noise performance, with relative intensity noise below 0.5% and phase fluctuations under 15 mrad. This new PM fiber platform provides a powerful tool for ultrafast metrology, coherent optical synthesis, and broadband light sources requiring exceptional stability and polarization control.

Keywords: Photonic crystal fibers, nonlinear optics, fibre optics, supercontinuum generation

1. INTRODUCTION

Broadband, low-noise light sources are essential for many applications in modern photonics, and supercontinuum generation (SCG) in all-normal dispersion (ANDi) optical fibres has emerged as a powerful solution [1–6]. ANDi SC sources provide spectrally flat, highly coherent light with excellent stability, making them particularly suitable for applications such as optical coherence tomography (OCT), nonlinear imaging, and dual-comb spectroscopy [7–9]. In contrast to soliton-based SCG, which is sensitive to noise through modulation instability, soliton interactions, and Raman effects, ANDi SCG is governed by self-phase modulation (SPM) and optical wave breaking (OWB), enabling deterministic and low-noise spectral broadening [1–4].

However, the performance of ANDi fibres can be limited by polarisation-related instabilities such as polarisation modulation instability (PMI) and stimulated Raman scattering (SRS) [10]. Polarisation-maintaining (PM) photonic crystal fibres (PCFs) have been developed to mitigate these effects, although conventional designs based on stress rods remain complex to fabricate [11].

Here, we propose a simplified PM-ANDi silica PCF design based on two enlarged air holes near the core, enabling robust polarisation maintenance without stress-applying elements. The fibre is engineered for near-zero dispersion around 1030 nm, making it well suited for pumping with Yb-based femtosecond lasers. We demonstrate broadband, flat SC spectra spanning 630–1350 nm using two different pump sources. The stability of the generated SC is assessed through dispersive Fourier transform measurements and phase-noise analysis, confirming excellent shot-to-shot coherence.

*Email T.S.: thibaut.sylvestre@umlp.fr

2. EXPERIMENT

Figure 1(a) shows the scanning electron microscope (SEM) image of the photonic crystal fiber (PCF) cross section, fabricated using a standard stack-and-draw process from silica capillaries. The structure comprises 11 rings of air holes, ensuring low confinement losses below a few dB/km up to 1300~nm (Fig.~1(b)). The fibre core diameter is 2.3~µm, with an air-filling fraction d/Λ=0.41, enabling single-mode operation across the supercontinuum bandwidth, as confirmed by the measured mode profile (inset of Fig.~1(b)). By optimizing the pitch (Λ=1.46 µm) and hole diameter (d1=0.58 µm), a smooth all-normal dispersion profile was achieved, with a minimum dispersion wavelength around 1010~nm. The dispersion for both slow and fast axes was obtained from finite-element simulations based on the SEM image and validated experimentally using a Mach–Zehnder interferometer and a broadband SC source, following the method of Ref. [12].

Polarization maintenance is achieved using two enlarged holes (d2=0.66 µm) placed near the core, yielding a phase birefringence of $\sim 2\times10^{-4}$ at 1030~nm (Fig.~1(c)). This approach avoids the use of stress rods, allowing a reduced fibre diameter (120~µm) and improved handling. The phase birefringence was obtained numerically, while the group birefringence was measured using a broadband polarimetric technique based on spectral interference between orthogonal polarization modes.

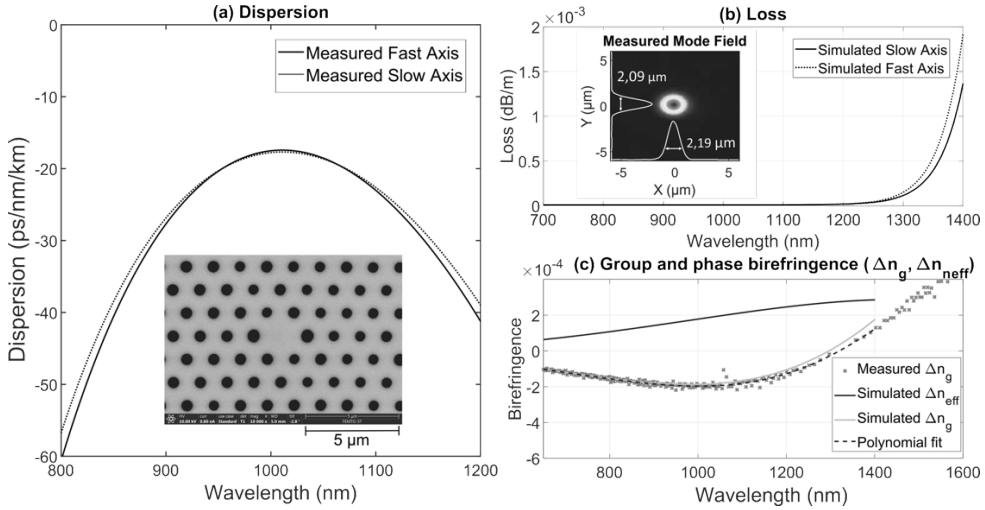

Figure 1. PM-ANDi PCF characterization: (a) Measured and simulated group-velocity dispersion (inset: SEM cross-section). (b) Simulated confinement losses (inset: mode profile). (c) Phase and group birefringence, measured vs. simulated.

3. RESULTS

3.1 Pumping at 1034 nm with 175 fs pulses

A 12.5 cm section of the drawn fibre was pumped with an Yb:YAG CPA femtosecond laser (Pharos PH1-SP-1mJ, 175 fs FWHM, 1034 nm). The output spectra were measured with an optical scanning spectrometer (APE waveScan). Figures 2(a)–(b) show SC spectra along the two polarization axes versus input peak power, comparing experiment (solid) and GNLSE simulations (dashed), which used the measured input spectrum (Fourier-limited, 175 fs). The numerical simulations were performed by solving the scalar generalized nonlinear Schrödinger equation (GNLSE) including quantum and technical (laser) noises [13,14]. Good agreement is observed, except in the infrared due to confinement losses. At 44 kW peak power (8 nJ pulses), the SC extends from 720–1300 nm (580 nm at –10 dB), with strong spectral modulations between 900–1100 nm, due to the impact of input pulse spectral shape on the SC output.

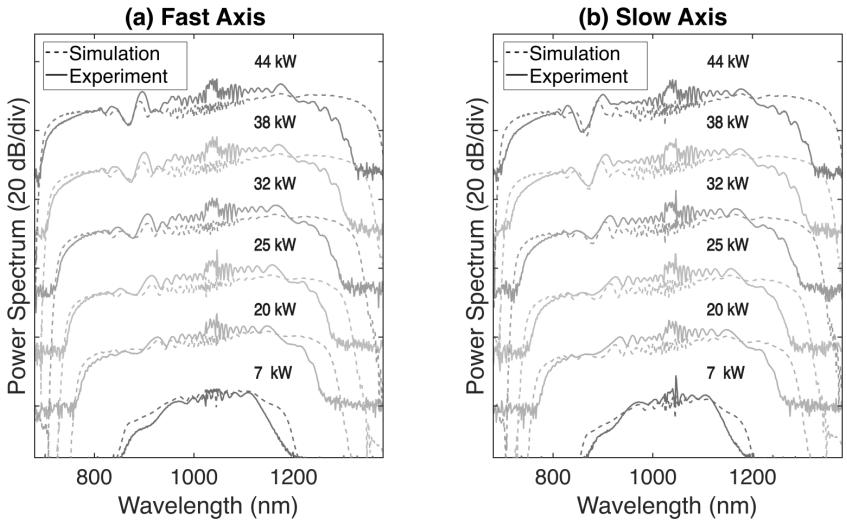

Figure 2. Experimental (solid) and numerical (dashed) ANDi-fibre output SC spectra (logarithmic scale, arbitrary units) along both fibre principal axes as a function of input pulse peak power, using a Ytterbium femtosecond laser pump at 1034 nm. All spectra are vertically shifted for improved clarity.

3.2 Pumping at 1030 nm with 120 fs pulses

A 20 cm functionalized PM-ANDi fibre with end-caps and connectors was then tested using a tunable Ti:Sapphire femtosecond laser (Coherent Chameleon Ultra II, 120 fs FWHM, near transform-limited pulses). Figure 4 shows the results at a pump wavelength of 1030 nm. The spectral ripples observed previously are significantly reduced, while the SC still spans 730–1300 nm. Numerical simulations using 120 fs sech² pulses (dashed lines) show excellent agreement with the measurements. At full coupling, the SC output power reaches 360 mW, corresponding to a spectral density of ~0.5 mW/nm.

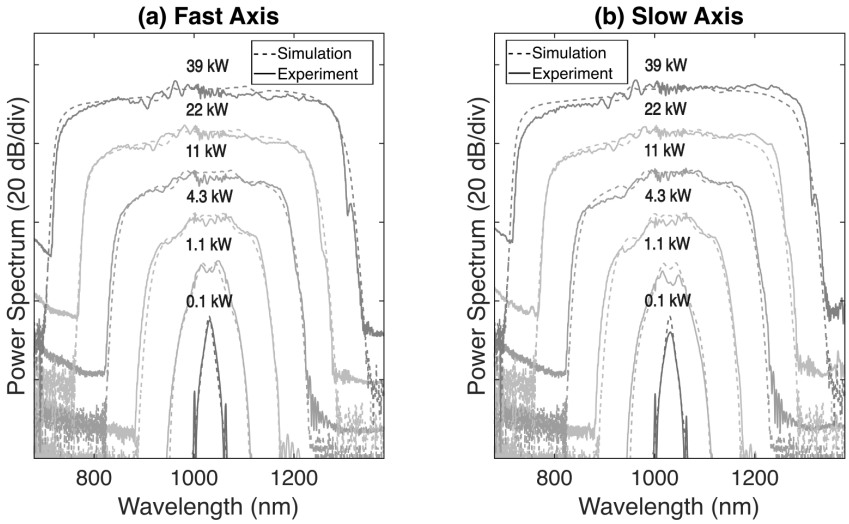

Figure 3. Experimental (solid) and numerical (dashed) fibre output SC spectra (logarithmic scale, arbitrary units) versus input peak power using a Ti:Sa femtosecond laser at 1030 nm when pumping the PM-ANDi fibre on (a) fast axis and (b) slow axis.

4. NOISE MEASUREMENTS

The stability and coherence of SC sources are essential for applications such as frequency metrology, spectroscopy, and imaging. SC generation in ANDi fibres is known for its low noise and high spectral coherence [1–6]. Here, we characterise the SC noise using two complementary approaches: (i) shot-to-shot relative intensity noise (RIN), and (ii) spectral phase fluctuations.

4.1 RELATIVE INTENSITY NOISE (RIN) MEASUREMENTS

Shot-to-shot spectral fluctuations were characterised using the dispersive Fourier transform (DFT) technique [15], which maps the SC spectrum into the time domain via propagation in a dispersive fibre. In our setup, a 232 m dispersion-shifted fibre (DSF, are β_2=36.5 ps^2/km and β_3=4.9 ps^3/km,) provided sufficient stretching for real-time spectral measurements with an effective resolution of ~8 nm. The temporally stretched signals were detected using a 5 GHz photodiode and a 12 GHz oscilloscope.

Figure 7(a) compares the averaged DFT spectra with OSA measurements, showing excellent agreement and validating the method. The relative intensity noise (RIN) was then extracted from the DFT data, with results shown in Fig. 7(b) for increasing input peak powers. RIN values remain as low as ~0.5% across most of the SC bandwidth, with higher noise at short wavelengths attributed to detector sensitivity and stretching fibre limitations.

To confirm these results, independent RIN measurements were performed without the stretching fibre using a tunable bandpass filter and statistical analysis of pulse-to-pulse fluctuations [13]. Good agreement is observed, especially at long wavelengths. Overall, the SC exhibits nearly constant low RIN, indicating the absence of significant noise amplification during generation.

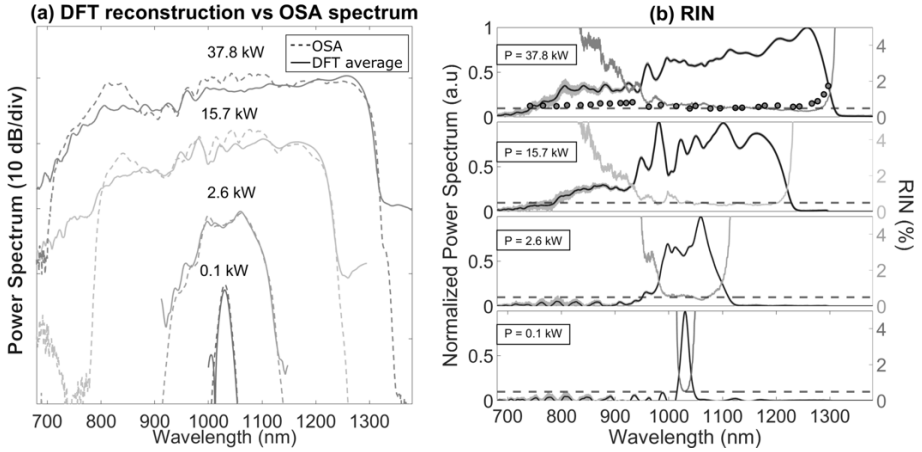

Figure 7. (a) Experimental (a) DFT spectra (solid) compared with OSA measurements (dashed) for increasing input peak power (fast axis). (b) Corresponding RIN spectra (colour). Grey lines show shot-to-shot fluctuations, black curves the averaged spectra. The dotted line indicates the 0.5% noise floor.

4.2 OPTICAL PHASE NOISE MEASUREMENTS

Phase noise was assessed using Bellini-Hänsch interferometry [16], by recording spectral interference between two SC sources in identical PM-ANDi fibers under the same pulse conditions. The setup, shown in Fig. 8(a), is a balanced Mach–Zehnder interferometer. Single-shot interference spectra were processed via a discrete Hilbert transform [17] to extract relative phase fluctuations versus shot number and wavelength. Analysis of 1000 consecutive spectra allowed quantification of statistical phase stability across the accessible bandwidth.

Figure 8(b) shows phase noise with a standard deviation of 8–15 mrad over 700–925 nm and 7–10 mrad over 1100–1330 nm. These results match a noise model (dashed line) including the interferometer's passive stability (~6 mrad rms

at 1030 nm) and shot/read noise effects (grey area). The measurements confirm that SC generation in PM-ANDi fibres is highly deterministic, with stochastic phase fluctuations below the detectable limit.

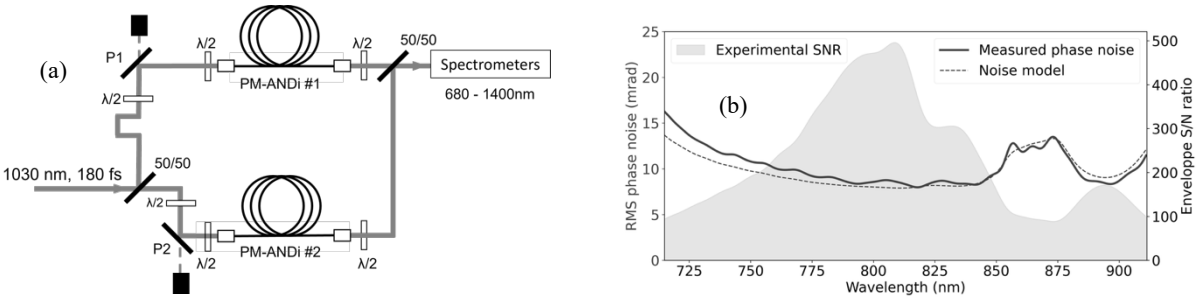

Figure 8. Optical phase noise measurements. (a) Interferometer setup with thin-film polarizers P1 and P2. (b) Relative phase noise of the two SCs (solid line) with model (dashed line); gray area shows SNR of the fringe envelope from 1000 single-shot measurements.

5. CONCLUSION

In conclusion, we demonstrate a simplified polarisation-maintaining all-normal-dispersion (PM-ANDi) photonic crystal fibre based on two enlarged central holes, removing the need for stress rods and enabling a compact 120 µm diameter. The fibre exhibits a near-parabolic dispersion around 1030 nm and generates broadband, flat supercontinua spanning 630–1350 nm. Its compatibility with different femtosecond sources and excellent noise performance highlight its potential for ultrafast photonics applications, including dual-comb spectroscopy, nonlinear imaging, and frequency comb technologies.

ACKNOWLEDGEMENTS

This work has received funding from the European Union's Horizon research and innovation program under grant agreements No. 101135904 (VISUAL project), from the French National Agency (ANR-17-EURE-0002), from the Région Bourgogne Franche-Comté, as well as the Institut Universitaire de France (IUF). Authors from PhLAM also acknowledge the Contrats de Plan Etat-Region (CPER WaveTech), the French Ministry of Higher-Education and Research, the Hauts-de-France (HdF) Regional Council, the European Regional Development Fund (ERDF), IRCICA and the FibreTech Lille technological platform.

REFERENCES

[1] Heidt, A. M., Hartung, A., Bosman, G. W., Krok, P., Rohwer, E. G., Schwoerer, H. & Bartelt, H. Coherent octave-spanning near-infrared and visible supercontinuum generation in all-normal dispersion photonic crystal fibers. *Opt. Express* **19**, 3775–3787 (2011). https://doi.org/10.1364/OE.19.003775

[2] Hooper, L. E., Mosley, P. J., Muir, A. C., Wadsworth, W. J. & Knight, J. C. Coherent supercontinuum generation in photonic crystal fiber with all-normal group velocity dispersion. *Opt. Express* **19**, 4902–4907 (2011). https://doi.org/10.1364/OE.19.004902

[3] Tarnowski, K., Martynkien, T., Mergo, P. et al. Compact all-fiber source of coherent linearly polarised octave-spanning supercontinuum based on normal-dispersion silica fiber. *Sci. Rep.* **9**, 12313 (2019). https://doi.org/10.1038/s41598-019-48812-3

[4] Heidt, A. M., Spangenberg, D. M., Rampur, A., Hartung, A. & Bartelt, H. All-normal dispersion fiber supercontinuum: Principles, design, and applications of a unique white light source. In R. R. Alfano (ed.) *The Supercontinuum Laser Source*, 299–341 (Springer, 2022). https://doi.org/10.1007/978-3-030-98722-5_7

[5] Sylvestre, T. et al. Recent advances in supercontinuum generation in specialty optical fibers. *J. Opt. Soc. Am. B* **38**(12), F90–F103 (2021). https://doi.org/10.1364/JOSAB.438806
[6] Dudley, J. M., Genty, G., Heidt, A., Sylvestre, T., Travers, J. C. & Taylor, J. R. Fibre supercontinuum generation: Progress and perspectives. *EPL* **151**, 55001 (2025). https://doi.org/10.1209/0295-5075/151/55001
[7] Rao, S. et al. Shot-noise limited, supercontinuum-based optical coherence tomography. *Light: Sci. & Appl.* **10**, 133–145 (2021). https://doi.org/10.1038/s41377-021-00591-0
[8] Rampur, A. et al. Perspective on the next generation of ultra-low noise fiber supercontinuum sources and their emerging applications in spectroscopy, imaging, and ultrafast photonics. *Appl. Phys. Lett.* **118**(24), 240504 (2021). https://doi.org/10.1063/5.0051881
[9] Newton, E., Jones, C., Hong, K.-H., Langseth, J. & Allured, R. Coherent combining of independently generated supercontinuum sources. Opt. Lett. 50, 6321–6324 (2025).
[10] Bravo Gonzalo, I., Engelsholm, R. D., Sørensen, M. P. et al. Polarisation noise places severe constraints on coherence of all-normal dispersion femtosecond supercontinuum generation. *Sci. Rep.* **8**, 6579 (2018). https://doi.org/10.1038/s41598-018-24959-8
[11] Genier, E. et al. Ultra-flat, low-noise, and linearly polarised fiber supercontinuum source covering 670–1390 nm. *Opt. Lett.* **46**, 1820–1823 (2021). https://doi.org/10.1364/OL.423656
[12] Hlubina, P., Kadulova, M. & Mergo, P. Chromatic dispersion measurement of holey fibres using a supercontinuum source and a dispersion-balanced interferometer. *Optics and Lasers in Engineering* **51**, 421–425 (2013). https://doi.org/10.1016/j.optlaseng.2012.10.009
[13] Agrawal, G. P. *Nonlinear Fiber Optics*. Academic Press (2019).
[14] Genier, E., Bowen, P., Sylvestre, T., Dudley, J. M., Moselund, P. & Bang, O. Amplitude noise and coherence degradation of femtosecond supercontinuum generation in all-normal-dispersion fibers. *J. Opt. Soc. Am. B* **36**, A161–A167 (2019). https://doi.org/10.1364/JOSAB.36.000A161
[15] Godin, T., Sader, L., Khodadad Kashi, A., Hanzard, P. H., Hideur, A., Moss, D. J., … Wetzel, B. (2022). Recent advances on time-stretch dispersive Fourier transform and its applications. *Advances in Physics: X*, *7*(1). https://doi.org/10.1080/23746149.2022.2067487
[16] Bellini, M. & Hänsch, T. W. Phase-locked white-light continuum pulses: toward a universal optical frequency-comb synthesizer. *Opt. Lett.* **25**(14), 1049–1051 (2000). https://doi.org/10.1364/OL.25.001049
[17] Maingot, B., Chériaux, G., & Jullien, A. Spectral coherence properties of continuum generation in bulk crystals. *Opt. Express* **30**, 20311–20320 (2022). https://doi.org/10.1364/OE.30.020311